Multivalued Synchronization by Poincaré Coupling

L. J. Ontañón-García[a], E. Campos-Cantón[b*], R. Femat[b],
I. Campos-Cantón[c], M. Bonilla-Marín[b]
[a]Instituto de Investigación en Comunicación Óptica,
Universidad Autónoma de San Luis Potosí, México.
[b]División de Matemáticas Aplicadas,
IPICYT, México.
[c]Facultad de Ciencias,
Universidad Autónoma de San Luis Potosí, México.

October 30, 2018

Abstract

This work presents multivalued chaotic synchronization via coupling based on the Poincaré plane. The coupling is carried out by an underdamped signal, triggered every crossing event of the trajectory of the master system through a previously defined Poincaré plane. A

*correspondence author: eric.campos@ipicyt.edu.mx

master-slave system is explored, and the synchronization between the systems is detected via the auxiliary system approach and the maximum conditional Lyapunov exponent. Due to the response to specific conditions two phenomena may be obtained: univalued and multivalued synchronization. Since the Lyapunov exponent is not enough to detect these two phenomena, the distance between the pieces of trajectories of the slave and auxiliary systems with different initial conditions is also used as a tool for the detection of multivalued synchronization. Computer simulations using the benchmark chaotic systems of Lorenz and Rössler are used to exemplify the approach proposed.
Keywords: chaos synchronization, Poincaré plane, multimodal synchronization.

1 Introduction

Coupled systems can be classified in two main categories: *Unidirectional-coupled systems*, formed by an autonomous master system whose trajectory constrains a slave system. *Bidirectional or mutual-coupled systems*, in which there is neither master nor slave system, but the two systems are constrained by the trajectory of each other. Synchronization phenomena in coupled systems have been extensively studied during the last decades and several concepts describing synchronized motions have been introduced [1, 2, 3]. Among them, we can mention: frequency entrainment [4], phase synchronization [5], lag synchronization [6], multimodal synchronization [7], complete (or full) synchronization [8], and forced synchronization [9].

In this work we focus only on the unidirectional-coupled scheme between

two chaotic systems. To make clear our purpose, let us consider the following master and slave systems:

$$\mathbf{x}' = \quad F(\mathbf{x}), \quad F : \mathbf{R}^m \to \mathbf{R}^m \tag{1}$$

$$\mathbf{y}' = \quad G(\mathbf{x}, \mathbf{y}), \quad G : \mathbf{R}^m \times \mathbf{R}^n \to \mathbf{R}^n \tag{2}$$

where the state vectors are represented by $\mathbf{x} \in \mathbf{R}^m$ and $\mathbf{y} \in \mathbf{R}^n$ with corresponding vector fields $F(\cdot)$ for the master system and $G(\cdot)$ for the slave system.

The coupled systems given by Eqs. (1) and (2) induce in the phase space $\mathbf{R}^m \times \mathbf{R}^n$ the flow $(\varphi^t)_{t\in\mathbf{R}}$. For each initial condition $(\mathbf{x}_0, \mathbf{y}_0)$ corresponds a trajectory given by $\{(\mathbf{x}(t), \mathbf{y}(t)) = \varphi^t(\mathbf{x}_0, \mathbf{y}_0) : t \geq 0\}$. If there exists a function $\varrho : \mathbf{R}^m \to \mathbf{R}^n$ for the pair of coupled systems, such that $\mathbf{y}(t) = \varrho(\mathbf{x}(t))$ for all $t \geq 0$, then it is said that the systems given by Eqs. (1) and (2) are synchronized see Rulkov *et al* [10]. If the distance between their states converges to zero along time (and hence ϱ is the identity function) then the systems (1) and (2) are said to present complete synchronization. However a weaker form of synchronization called Generalized Synchronization (GS) allows the coupled systems to have an arbitrary distance between their states, therein ϱ results in a more complicated relation than the identity function.

In order to ease the analysis and detection of GS between master and slave systems, the auxiliary system approach was presented by Abarbanel *et al* in [11]. Here is considered an auxiliary system identical to the slave system, and coupled in the same way to the master system, but with different set of initial conditions $\mathbf{z}_0 \neq \mathbf{y}_0$. Synchronization between states of master and slave systems can be easily detected by this method if the coupled systems

present only one basin of attraction and the following asymptotic condition is satisfied:

$$\lim_{t\to\infty} \|\mathbf{y}(t) - \varrho(\mathbf{x}(t))\| \to 0. \tag{3}$$

But if there are N multiple basins of attraction $\mathcal{D}_1, \mathcal{D}_2, \ldots, \mathcal{D}_N$ then the ϱ function is given by:

$$\varrho(\mathbf{x}(t)) = \begin{cases} \varrho_1(\mathbf{x}(t)) & \text{if } (\mathbf{x}_0, \mathbf{y}_0) \in \mathcal{D}_1 \\ \varrho_2(\mathbf{x}(t)) & \text{if } (\mathbf{x}_0, \mathbf{y}_0) \in \mathcal{D}_2 \\ \vdots & \\ \varrho_N(\mathbf{x}(t)) & \text{if } (\mathbf{x}_0, \mathbf{y}_0) \in \mathcal{D}_N \end{cases} \tag{4}$$

So there are $\varrho_i(\mathbf{x}(t)), i = 1, 2, ..., N$ different functions where N stands for the number of basins of attraction. Thus, if the coupled systems present one or more than one basin of attraction ($N \geq 1$), two situations are possible. If there exists only one basin of attraction and GS is ensured, $\lim_{t\to\infty} \|\mathbf{y}(t) - \mathbf{z}(t)\| \to 0$ is satisfied for any initial state $\mathbf{y}_0$ and $\mathbf{z}_0$, which means that the slave and auxiliary systems are initialized with $\mathbf{y}_0$ and $\mathbf{z}_0$ such that their trajectories converge in the same attractor. Complementarily, if there exist more than one basin of attraction and GS is ensured, we have that Eq. (3) implies: (i) $\lim_{t\to\infty} \|\mathbf{y}(t) - \mathbf{z}(t)\| \to 0$ is satisfied for any initial conditions $\mathbf{y}_0$ and $\mathbf{z}_0$ belonging to the same basin of attraction and (ii) $\lim_{t\to\infty} \|\mathbf{y}(t) - \mathbf{z}(t)\| \to d > 0$, if d exists, for initial conditions $\mathbf{y}_0$ and $\mathbf{z}_0$ belonging to distinct basin of attraction.

It is worth mentioning that the Maximum Conditional Lyapunov Exponent (MCLE) is always negative when the master-slave system is synchro-

nized but it cannot detect multivalued synchronization. So, it is relevant to use in combination with the former the auxiliary system to detect whether the synchronization is multivalued.

In this paper we suppose that the function G in Eq. (2) has the classical form $G(\mathbf{x}, \mathbf{y}) = G_a(\mathbf{y}) + K[u(\mathbf{x}) - G_c(\mathbf{y})]$ (see [3, 12]). Where G_a is the autonomous part of the dynamics of the slave system, $K = (k_{ij})_{1 \leq i,j \leq n} \in M_n(\mathbf{R})$ is a real square matrix of size n whose coefficients rule the dissipative coupling, $u : \mathbf{R}^m \to \mathbf{R}^n$ is a function of the state vector of the master system and $G_c : \mathbf{R}^n \to \mathbf{R}^n$ is a function of the state vector of the slave system which acts as a feedback.

In most studies (see [1, 2, 3] and the references within) the function G is a continuous function of $\mathbf{x}$ and $\mathbf{y}$ which does not depend on time. Nevertheless, time dependent couplings appear in real systems such as biological networks [13, 14, 15].

For example, in integrate and fire neural networks [16], neurons interact only at the instants when their membrane potential reaches some threshold, and it has been observed [17] that pancreatic beta cells networks synchronize at specific periods of time by the increase or decrease of substances such as intracellular calcium [18]. The thresholds associated to each neuron may define a Poincaré section in the phase space of the network, and the neurons interact only when an orbit of network crosses this section

With this in consideration, here we introduce the concept of coupling based on a Poincaré plane. Such coupling is activated whenever the trajectory of the master system crosses the Poincaré plane, generating complex driving signals that do not depend continuously on the state of the master system.

That is, the coupling is a function of time $K[H_1(\mathbf{x},t)-H_2(\mathbf{y},t)]$. Here we will suppose that the driving signal H_1 is triggered by a threshold, and its shape is defined by the combination of two signals: the first, is a signal defined as a function of time and activated each time the trajectory of the master system crosses the Poincaré plane, and the second is the state of the master system. The term H_2, is a function of the state vector of the slave system and the time. This type of coupling in contrast to more traditional approaches is not continuous in general. Here the Poincaré plane monitors the master system but perturbs the slave system unlike the OGY [19] which monitors and perturbs only the latter.

The paper is organized as follows: In the section 2 the coupling based on Poincaré plane is presented; the section 3 contains numerical results about master-slave interconnection; finally, conclusions are made in section 4.

2 Coupling based on Poincaré plane

In order to define the coupling presented in this work, we assume the master slave systems given by Eqs. (1) and (2) have a dissipation ball $\mathcal{D} \subset \mathbf{R}^m \times \mathbf{R}^n$, such that $\varphi^t(\mathcal{D}) \subset \mathcal{D}$ for all $t \geq 0$. This dissipation ball is of the form $\mathcal{D} = \mathcal{D}_x \times \mathcal{D}_y$. The maximal attractor $\mathcal{A}$ is the largest attracting invariant subset of $\mathcal{D}$, with projection $\mathcal{A}_x := \prod_x \mathcal{A}$ into $\mathbf{R}^m$ and projection $\mathcal{A}_y := \prod_y \mathcal{A}$ into $\mathbf{R}^n$. The flow restricted to $\mathcal{A}_x$ is denoted as $\varphi_m^t := \varphi^t|\mathcal{A}_x$ and $\mathbf{x}(t) := \varphi_m^t(\mathbf{x}_0)$. For further convenience, let us define $\varphi_s^t := \prod_y \circ \varphi^t$ and $\mathbf{y}(t) := \varphi_s^t(\mathbf{x}_0, \mathbf{y}_0)$.

First, we define a Poincaré plane as $\Sigma := \{(x_1, \ldots, x_m) \in \mathbf{R}^m : \alpha_1 x_1 + \alpha_2 x_2 + \ldots + \alpha_m x_m + \alpha_{m+1} = 0\}$, where $\alpha_1, \ldots, \alpha_{m+1} \in \mathbf{R}$ are coefficients of a

hyperplane equation whose values are considered according to the following rationale. The Poincaré plane must be located to guarantee $\mathcal{A}_x \bigcap \Sigma \neq \emptyset$, which is satisfied if $\mathcal{A}_x \bigcap \Sigma$ has at least one element $\mathbf{x}^* = \varphi_m^{t_0}(\mathbf{x}_0)$. We are interested in several crossing events $\{\varphi_m^{t_0}(\mathbf{x}_0),\ \varphi_m^{t_1}(\mathbf{x}_0),\ \varphi_m^{t_2}(\mathbf{x}_0),\ \ldots\} \in \Sigma$ and therefore specify the following time series $\Delta_{\mathbf{x}_0} = \{t_0, t_1, t_2, \ldots\}$, which depends on the initial conditions of the master system. Then for each $\mathbf{x}_0 \in \mathcal{A}_x$, there exists an infinitely large number of different positive times t_k for which $\#\Delta_{\mathbf{x}_0} \to \infty$ when $t \to \infty$, where $\#\Delta_{\mathbf{x}_0}$ means the cardinality of the set $\Delta_{\mathbf{x}_0}$. In such a case, it will exist an increasing sequence $\{t_k(\mathbf{x}_0)\}_{k\in\mathbf{N}}$ such that $\varphi_m^{t_0(\mathbf{x}_0)}(\mathbf{x}_0) = \mathbf{x}^* \in \Sigma$ for all $k \in \mathbf{N}$. Henceforth, we assume the following:

(a) The Poincaré plane must be located in order to meet the condition $\mathcal{A}_x \bigcap \Sigma \neq \emptyset$.

(b) The master system given by Eq. (1) oscillates in a chaotic regimen. Then, for each $\mathbf{x}_0 \in \mathcal{A}_x$, there exists an infinitely large number of different positive times t_k for which $\#\Delta_{\mathbf{x}_0} \to \infty$ when $t \to \infty$, *i.e.*, for $\varphi_m^{t_0}(\mathbf{x}_0) = \mathbf{x}^* \in \Sigma$, there is a time t_1 such that $\mathbf{x}(t_1) := \varphi_m^{t_1}(\mathbf{x}^*) \in \Sigma$, next there is a time t_2 such that $\mathbf{x}(t_2) := \varphi_m^{t_2}(\mathbf{x}^*) \in \Sigma$ and so forth.

Having this in consideration we define the Poincaré coupling:

Definition 2.1. *Let $\boldsymbol{x}_0$ be a point in the phase space of the master system and $\Delta_{x_0} = \{t_0, t_1, t_2, \ldots\}$ be a time series comprised of the events generated each time that the trajectory of the master system with initial condition $\boldsymbol{x}_0$ crosses the Poincaré plane Σ. If the coupling $K[H_1(\boldsymbol{x}, t) - H_2(\boldsymbol{y}, t)]$ depends on the time series $\Delta_{\mathbf{x}_0}$ then the coupling is called a Poincaré coupling.*

Now, we further specify the equation of the slave system, which takes the following form:

$$\mathbf{y}' = G_a(\mathbf{y}) + K[H_1(\mathbf{x}, t) - H_2(\mathbf{y}, t)]. \tag{5}$$

The coupling is given by the second term of the right hand side with the corresponding functions $H_1(\mathbf{x}, t) = h_1(t)u(\mathbf{x})$, and $H_2(\mathbf{y}, t) = h_2(t)G_c(\mathbf{y})$.

Where h_1 refers to a $n \times n$ time-dependent real matrix containing sliding functions $S_{pq}(t) : \mathbf{R} \to \mathbf{R}$ which are triggered each time that the trajectory of the master system $\mathbf{x}(t)$ crosses the Poincaré plane Σ, *i.e.* each time $t_i \in \Delta_{\mathbf{x}_0}$. The matrix is given as follows:

$$h_1(t) = \begin{pmatrix} S_{11}(t) & S_{12}(t) & \dots & S_{1n}(t) \\ S_{21}(t) & S_{22}(t) & \dots & S_{2n}(t) \\ \vdots & \vdots & \ddots & \vdots \\ S_{n1}(t) & S_{n2}(t) & \dots & S_{nn}(t) \end{pmatrix} \tag{6}$$

where each entry $S_{pq}(t)$ can be defined according to specific requirements for the coupling signal, with $p, q = 1, \dots, n$, and it is formed as $S_{pq}(t) = S^1_{pq}(t) + S^2_{pq}(t) + S^3_{pq}(t) + \dots$, where each element takes the following form:

$$S^i_{pq}(t) = \begin{cases} S_{pq}(t - t_i) & t \in [t_i, t_{i+1}), \text{ with } t_i \in \Delta_{\mathbf{x_0}}, \\ 0 & \text{otherwise}, \end{cases} \tag{7}$$

where S_{pq} is a scalar function which is defined in a given interval. The function h_2 may be defined in a similar way or as a constant, making the feedback continuous.

Now, we are interested in studying GS between a pair of chaotic systems, either identical or different, coupled by distinct H_1 matrix with different coefficients of the coupling strength K.

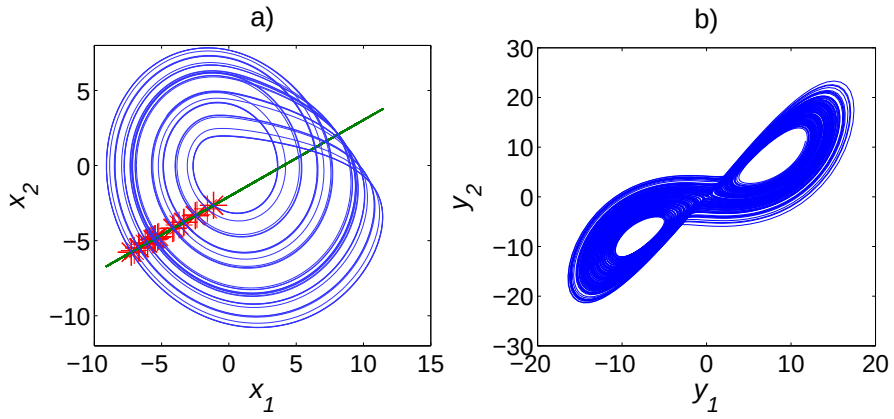

Figure 1: a) Projection of the attractor of the Rössler system onto the (x_1, x_2) plane intersected by the Poincaré plane given by Eq. (16). The point of each crossing event within $\{\varphi_m^{t_0}(\mathbf{x}_0), \varphi_m^{t_1}(\mathbf{x}_0), \varphi_m^{t_2}(\mathbf{x}_0), \dots\}$ is marked with asterisk. b) Projection of the attractor of the Lorenz system onto the (y_1, y_2) plane.

3 Multivalued synchronization by Poincaré coupling

In this section we present a descriptive example of the synchronization phenomenon, based on the Poincaré coupling which can be explored with identical or different systems. Our concept of Poincaré coupling is illustrated by synchronizing two benchmark systems. The Rössler system is given by:

$$\begin{aligned} \dot{x}_1 &= -x_2 - x_3, \\ \dot{x}_2 &= x_1 + a x_2, \\ \dot{x}_3 &= b + x_3(x_1 - c), \end{aligned} \tag{8}$$

where $(x_1, x_2, x_3)^T \in \mathbf{R}^3$ is the state of the system, and for which we take

the parameter values $a = 0.2$, $b = 0.2$ and $c = 5.7$ that locate the system in the chaotic regime. Figure 1 a) shows a projection of the attractor of the Rössler system onto the (x_1, x_2) plane. The Lorenz system is given by:

$$\begin{aligned} \dot{y}_1 &= \sigma(y_2 - y_1), \\ \dot{y}_2 &= \rho y_1 - y_2 - y_1 y_3, \\ \dot{y}_3 &= y_1 y_2 - \beta y_3, \end{aligned} \tag{9}$$

where $(y_1, y_2, y_3)^T \in \mathbf{R}^3$ is the state of the system, and the parameters values $\sigma = 10$, $\rho = 25$ and $\beta = 8/3$ are taken in such way that the system is also located in the chaotic regime. Figure 1 b) shows a projection of the attractor of the Lorenz system onto the (y_1, y_2) plane. The equilibria of the Lorenz system is given by:

$$Q = (\ \ 0, \quad 0, \quad 0\ \ ), \tag{10}$$

$$R = (\quad \eta, \quad \eta, \quad \mu\quad), \tag{11}$$

$$S = (\quad -\eta, \ -\eta, \ \mu\quad), \tag{12}$$

where $\eta = \sqrt{\beta\,(\sigma - 1)}$ and $\mu = \rho - 1$.

Although the coupling signal can be generated in several ways, for simplicity we deemed only one case concerning the matrix K, h_1 and h_2 as follows:

$$K = \begin{pmatrix} k_{11} & 0 & 0 \\ 0 & 0 & 0 \\ 0 & 0 & 0 \end{pmatrix}, h_1(t) = \begin{pmatrix} S_{11}(t) & 0 & 0 \\ 0 & 0 & 0 \\ 0 & 0 & 0 \end{pmatrix}, h_2(t) = \begin{pmatrix} 1 & 0 & 0 \\ 0 & 0 & 0 \\ 0 & 0 & 0 \end{pmatrix} \tag{13}$$

where the coupling strength is given by the scalar $k_{11} \geq 0$. The terms $u(\mathbf{x})$ and $S_{11}(t)$ from Eq. (5) are determined by Eqs. (6) and (7) as follows:

$$u(\mathbf{x}) = (x_1, 0, 0)^T; \tag{14}$$

$$S_{11}(t) = \begin{cases} e^{-\tau(t-t_i)} & t \in [t_i, t_{i+1}); \\ 0 & \text{otherwise}, \end{cases} \tag{15}$$

where $0 \leq \tau \in \mathbf{R}$ represents an underdamping factor which allows us to modulate the magnitude of signal and its frequency. Note that for a value of $\tau = 0$, the coupling becomes the negative feedback from the classical form described above [12], and that the signal $S_{11}(t)$ is triggered each time the master system trajectory crosses the Poincaré plane (see Figure 1 a)). The equation of the Poincaré plane implemented for the coupling is given as follows:

$$\Sigma := \{(x_1, x_2, x_3) : \alpha_1 x_1 + \alpha_2 x_2 + \alpha_3 x_3 + \alpha_4 = 0\}. \tag{16}$$

In order to meet the requirements of the plane from the discussion in Section 2, the parameters take the following values $\alpha_1 = 0.5934, \alpha_2 = -1.1636, \alpha_3 = 0, \alpha_4 = -2.4068$, and so the condition $\mathcal{A}_x \bigcap \Sigma \neq \emptyset$ is fulfilled. Figure 1 a) depicts the projection of the orbit of the master system onto the (x_1, x_2) plane intersected by Eq. (16). For this particular case we have focused on the crossing events of the trajectory of the master system with Σ in only one direction. So the time series $\Delta_{\mathbf{x}_0}$ contains each crossing event that satisfy $\frac{dx_1}{dt} > 0$. Figure 2 depicts the signal of Eq. (15) and the component $y_1(t)$ of the slave system with the autonomous part taken as the Lorenz system. Indeed the Eq. (5) for the slave system results as follows:

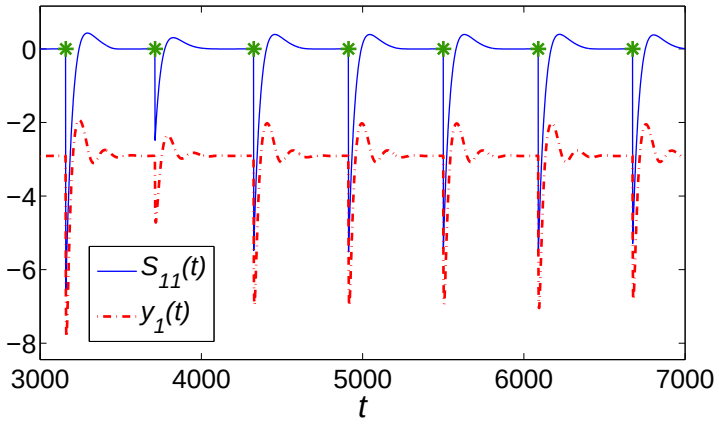

Figure 2: Signal $S_{11}(t)$ from Eq. (15) in solid line, and the component $y_1(t)$ of the slave system in dashed line for $\tau = 0.018, k_{11} = 50$. Marked with asterisk the events t_i of each intersection of the master system with the plane Σ (see Figure 1 a)).

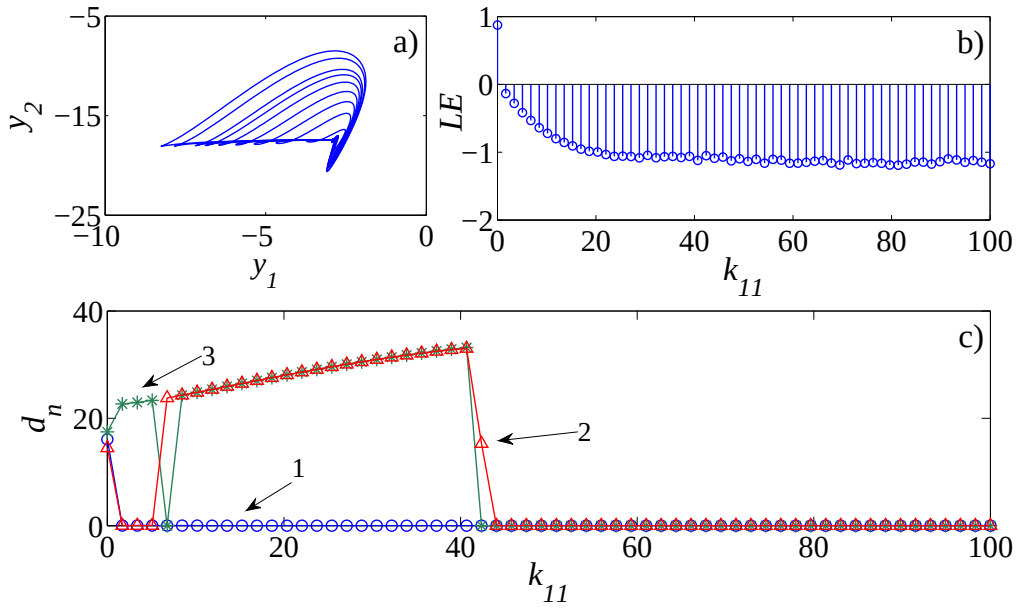

Figure 3: Unidirectional coupling with Rössler-Lorenz systems. a) Projection of the attractor of the slave system onto the (y_1, y_2) plane for $k_{11} = 50, \tau = 0.018$. b) Maximum conditional Lyapunov exponent. c) Distance d_n between the pieces of trajectories of the slave and auxiliary systems with different initial conditions against parameter k_{11}.

$$\mathbf{y}' = \begin{bmatrix} \dot{y}_1 \\ \dot{y}_2 \\ \dot{y}_3 \end{bmatrix} + k_{11} \begin{bmatrix} x_1 e^{-\tau(t-t_i)} - y_1 \\ 0 \\ 0 \end{bmatrix}. \tag{17}$$

The master, slave, and auxiliary systems are initialized with the different initial conditions given by $\mathbf{x}_0 = (-1.1, 1.15,\ 0.6116)$, $\mathbf{y}_0 = (7,\ 8,\ 24)$, and $\mathbf{z}_0 = (1,\ 1,\ 1)$, respectively.

Figure 3 a) shows the projection of the attractor of the Lorenz slave

system onto the plane (y_1, y_2). For $k_{11} = 50$, this attractor presents only oscillations around the equilibrium point S in contrast to the Lorenz system which is depicted in Figure 1 b) and Figure 2) shows the behavior of the y_1 component along time. The form of the attractor hinges on the coupling strength and the Poincaré section chosen, that is, whether the slope is greater or smaller.

Stability of the synchronization motion is a very relevant issue, and many criteria have been established in the literature to cope with it. One of the most popular and widely used criterion is the use of the Lyapunov exponents as average measurements of expansion or shrinkage of small displacements along the synchronized trajectory. In the context of master-slave systems the MCLE is used, this exponent is shown in Figure 3 b). It is important to emphasize that the negativity of the MCLE is only a necessary condition for stability of synchronized state, and that it is obtained from a temporal average, therefore they characterize the global stability over the whole chaotic attractor. However, this exponent is not a sufficient condition to determine synchronization, in some cases the MCLE may be negative and yet the systems are not synchronized [20]. Thus additional conditions should be fulfilled to warrant synchronization in a necessary and sufficient way, therein we have used the auxiliary system approach. In this way a second criteria for GS is the distance between slave and auxiliary systems which is a function of $\mathbf{R}^3 \times \mathbf{R}^3 \rightarrow \mathbf{R}^+$, *i.e.*, $d_n\left(\{\mathbf{y}(i)\}_{i\in\{1,\ldots,n\}}, \{\mathbf{z}(i)\}_{i\in\{1,\ldots,n\}}\right) = \frac{1}{n}\sum_{i=1}^{n} \|\mathbf{y}(i) - \mathbf{z}(i)\|$, with the Euclidean norm where n stands for the number of iterations in the numerical simulation made with a fourth-order Runge Kutta method. For this case we considered $n = 100000$ iterations after the transient regime. Figure 3 c)

shows the distance d_n against k_{11} when the slave and the auxiliary systems are initialized with $\mathbf{y}_0$ and $\mathbf{z}_0$, respectively. In line "1" marked with circles, d_n goes to zero as k_{11} increases indicating that the slave system is synchronized with the master system. If we change the initial condition for the slave system $(-7, -8, 24)$ and keep the same $\mathbf{z}_0$ for the auxiliary system, an interesting behavior for the distance d_n is detected, *i.e.*, there are values for k_{11} that makes $d_n \neq 0$ and correspond to GS of master-slave system, see Figure 3 c) line "2" marked with triangles. Line "3" marked with asterisk presents a similar phenomenon by changing $\mathbf{y}_0 = (-4.29, -13.01, 0.6116)$. Note that for a value of $k_{11} \approx 7$, the distance $d_n = 0$. This is due to the existence of multiple basin of attraction. Therefore, there are two asymptotic behaviors and d_n is an indicator of this. So we define such phenomena as follows:

Definition 3.1. *Let $k_{11} \in \mathcal{I} \subset \mathbf{R}$ be the coupling strength ensuring the GS of the master-slave system. Let us denote $d_n\left(\{\boldsymbol{y}(i)\}_{i\in\{1,\dots,n\}}, \{\boldsymbol{z}(i)\}_{i\in\{1,\dots,n\}}\right) = \frac{1}{n}\sum_{i=1}^{n} \|\boldsymbol{y}(i) - \boldsymbol{z}(i)\|$ as the distance between the pieces of trajectories of the slave and auxiliary system initialized at $\boldsymbol{y}_0, \boldsymbol{z}_0 \in \mathcal{D} = \bigcup_{i=1}^{N} \mathcal{D}_i$, respectively:*
(i)If $d_n = 0$ for all $\boldsymbol{y}_0, \boldsymbol{z}_0 \in \mathcal{D}$, then the GS of the master-slave system is said to be in a univalued mode.
(ii)If $d_n = 0$ for $\boldsymbol{z}_0 \in \mathcal{D}_j$ and $d_n \neq 0$ for $\boldsymbol{z}_0 \in \mathcal{D}_l$, with $j \neq l$, $\boldsymbol{y}_0 \in \mathcal{D}_j$, then the GS of the master-slave system is said to be in a multivalued mode.

According to the above definition, the GS of the master-salve system has two modes: univalued and multivalued. The univalued synchronization mode is found for $k_{11} > 45$ with the overlapping of lines "1", "2" and "3" in Figure 3 c). The coupling strength is such that makes the trajectories of the slave and auxiliary systems converge to the same basin of attraction for

all $\mathbf{y}_0, \mathbf{z}_0 \in \mathcal{D}$. Now, for simplicity, multivalued synchronization is illustrated with the bivalued case, i.e., the case of two basin of attraction. The bivalued synchronization mode is found in the interval $0.2 < k_{11} < 45$ where two basins of attraction exist; see Figure 3 c). These basins are interpreted as the coexistence of bistable equilibrium states for the same set of system parameter values than univalued but for a distinct coupling strength. That is, the emergence of bistability depends sensitively on the coupling strength.

We now detail what is hidden behind Figure 3 c). Considering $x_1 = 0$ in Eq. (17) to study the stability of the equilibria as a function of the k_{11} coupling strength. Note that the equilibrium point Q, given by Eq. (10), always exists independently of the value of k_{11}. However the equilibria R and S, given by Eqs. (11) and (12), respectively, depend on the value of the coupling strength. These last equilibria can be written as a function of k_{11} as follows: $\eta = \sqrt{\beta\left(\frac{\sigma\rho}{\sigma+k_{11}} - 1\right)}$ and $\mu = \frac{(\sigma+k_{11})}{\sigma}$. As k_{11} tends to increase, the equilibrium points R and S start to approach symmetrically to the point Q. The system given in Eq. (17) presents negative eigenvalues in the symmetrical points R and S, meaning that any trajectory near this points will be attracted to them, causing bistability. Each equilibrium point R and S has its basin of attraction and these basins are symmetrically provided due to the slave systems is symmetric under the transformation $(y_1, y_2, y_3) \to (-y_1, -y_2, y_3)$. This fact suggests that if slave system displays a non-symmetric attractor then the basins of attraction might be non-symmetric.

The effect of the symmetry appearing at the boundaries of the basin of attraction is exemplified in Figure 4; where k_{11} takes the value of 3.6. The basins of attraction present a complex interlaced structure in all the

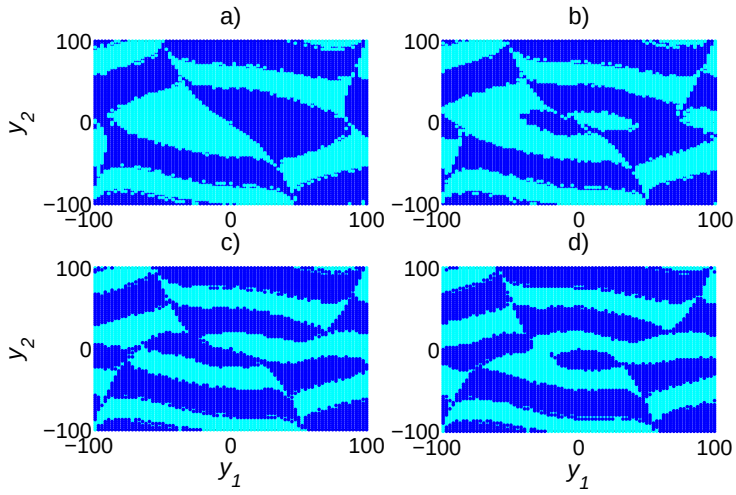

Figure 4: Two basins of attraction marked with the areas in blue and cyan for $k_{11} = 3.6$ which are two dimensional sections of the three-dimensional state space onto the planes: a) $y_3 = 0$, b) $y_3 = 10$, c) $y_3 = 20$, and d) $y_3 = 30$.

three-dimensional state space as is shown in Figure 4a), b), c) and d) onto different planes. For the coupling strength $k_{11} = 20$, the master system leads the response systems to have different boundaries of the basin of attraction as is depicted in Figure 5 a), b), c) and d) onto different planes. Comparing the basins of attraction for the plane $y_3 = 0$ from Figures 4 a) and 5 a), with $k_{11} = 3.6$ and $k_{11} = 20$, respectively, one is able to perceive the change at the boundaries of the basins of attraction due to the coupling strength. The basins of attraction have been determined considering 10000 iterations in the numerical simulation. For a value of $k_{11} > 45$ and for all $\mathbf{y}_0, \mathbf{z}_0 \in \mathcal{D}$, the GS of the master-slave system is in an univalued mode, *i.e.*, there is only one basin of attraction.

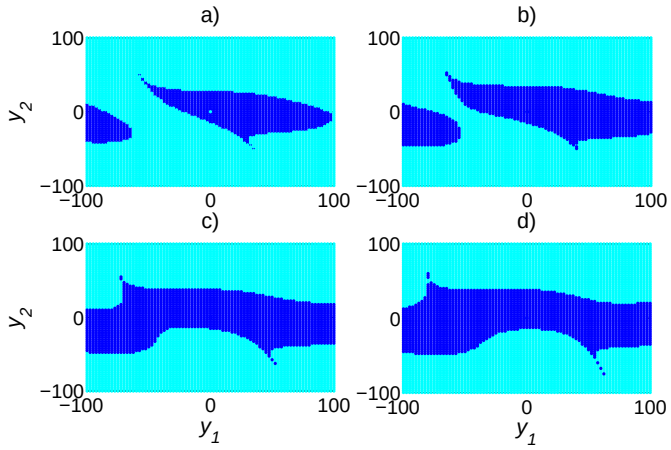

Figure 5: Two basins of attraction marked with the areas in blue and cyan for $k_{11} = 20$ which are two dimensional sections of the three-dimensional state space onto the planes: a) $y_3 = 0$, b) $y_3 = 10$, c) $y_3 = 20$, and d) $y_3 = 30$.

4 Concluding remarks

A Poincaré plane is traditionally used as a characterization tool for time series of nonlinear systems. Here, we have employed it to induce synchronization between different chaotic systems triggering a coupling signal each time the trajectory of the master system crosses the plane. So, the concept of Poincaré coupling has been introduced, generating driving signals that do not depend continuously on the state of the master system. A master-slave system was explored by using as benchmark. This configuration leads to multivalued synchronization phenomena depending on the strength of coupling expressed by the parameter k_{11}. We show the univalued or bivalued synchronization modes. For the bivalued synchronization mode, the symmetric curves appearing at the boundaries of the basins of attraction (commonly at-

tributed to multivalued synchronization, see [20]) hinge on the symmetry of the slave system. The maximal conditional Lyapunov exponent does not detect multivalued synchrony in a master-slave system. However, the distance between the pieces of trajectories with different initial conditions is key to determine the multivalued synchronization phenomenon. Future investigations might be opened towards the possible multivalued synchronization in biological systems. Results in this direction would be reported elsewhere.

Acknowledgments

The authors thank the anonymous reviewers for their pertinent suggestions to improve this work. L.J.O.G. is a doctoral fellow of Conacyt in the Graduate Program on Applied Science at IICO-UASLP. E.C.C. acknowledges CONACYT for the financial support through project No. 181002.

References

[1] S. Boccaletti, J. Kurths, G. Osipov, D. L. Valladares, The synchronization of chaotic systems, Physics Reports **366**, (2002), 1–101.

[2] A. C. J. Luo, A theory for synchronization of dynamical systems, Commun. Nonlinear Sci. Numer. Simulat., **14**, (2009) 1901–1951.

[3] A. Pikovsky, M. Rosenblum and J. Kurths, Synchronization: A universal concept in nonlinear sciences, Cambridge Nonlinear Sciences Series **12**, (2001).

[4] V.S. Anischenko, T.E. Vadivasova. D.E. Postnov and M.A. Safonova, Synchronization of chaos, Int. J. Bif. and Chaos, **2**, (1992) 633–644.

[5] M.G. Rosenblum, A.S. Pikovsky and J. Kurths, Phase synchronization of chaotic oscillators, Phys. Rev. Lett. **76**, (1996) 1804–1807.

[6] M.G. Rosenblum, A.S. Pikovsky and J. Kurths, From phase to lag synchronization in coupled chaotic oscillators, Phys. Rev. Lett. **78**, (1997) 4193–4196.

[7] E. Campos, J. Urias and N.F. Rulkov, Multimodal synchronization of chaos, Chaos, **14**, (2004) 48–54.

[8] L.M. Pecora and T.L. Carroll, Synchronization in chaotic systems, Phys. Rev. Lett. **64**, (1990) 821–824.

[9] J.S. González-Salas, E. Campos-Cantón, F.C. Ordaz-Salazar and I. Campos-Cantón, Forced synchronization of a self-sustained chaotic oscillator, Chaos, **18**, (2008) 023136.

[10] N.F. Rulkov, M.M. Sushchik, L.S. Tsimring, and H.D.I. Abarbanel, Generalized syncrhonization of chaos in directionally coupled chaotic systems, Phys. Rev. E **51**, (1995) 980–993.

[11] H.D.I. Abarbanel, N.F. Rulkov and M.M. Sushchik, Generalized synchronization of chaos: the auxiliary system approach, Phys. Rev. E **53**, (1996) 4528–4535.

[12] T. Kapitaniak, Synchronization of chaos using continous control, Phys. Rev. E **50**, (1994) 1642–1644.

[13] C. Stokes and J. Rinzel, Diffusion of extracellular K^+ can synchronize bursting oscillations in a model islet of Langerhans, Biophys. J., **65**, (1993) 597–607.

[14] E.M. Izhikevich, Weakly pulsed-coupled oscillators FM interactions, synchronization, and oscilatory associative memory, IEEE Transactions on neural networks, **10**, (1999) 508–526.

[15] E. Mirollo and S. Strogatz, Synchronization of pulsed-coupled biological oscillators, SIAM J. Appl. Math, **10**, (1990) 1645–1662.

[16] N. Brunel and V. Hakim, Fast Global Oscillations in Networks of Integrate-and-Fire Neurons with Low Firing, Neural Computation **11**, 1621–1671 (1999).

[17] P. Meda, I. Atwater, A. Gonçalves, A. Bangham, L. Orci and E. Rojas, The topography of electrical synchrony among β-cells in the mouse islet of Langerhans, Quarterly journal of experimental physiology, **69**, (1984) 719–735.

[18] L.J. Ontañón-García, E. Campos-Cantón, Discrete coupling and synchronization in the insulin release in the mathematical model of the β cells, Discrete dynamics in nature and society, (2013), in press.

[19] E. Ott, C. Grebogi and J. Yorke, Controlling chaos, Phys. Rev. Lett. **64**, (1990) 1194–1199.

[20] J.M. González-Miranda, Synchronization of symmetric chaotic systems, Phys. Rev. E **53**, (1996) 5656–5669.